SEUNG-HYEOK SHIN[1], SANG-GYU KIM[1], BYOUNGCHUL HWANG[1*]

APPLICATION OF ARTIFICIAL NEURAL NETWORK TO PREDICT THE TENSILE PROPERTIES OF DUAL-PHASE STEELS

An artificial neural network (ANN) model was developed to predict the tensile properties of dual-phase steels in terms of alloying elements and microstructural factors. The developed ANN model was confirmed to be more reasonable than the multiple linear regression model to predict the tensile properties. In addition, the 3D contour maps and an average index of the relative importance calculated by the developed ANN model, demonstrated the importance of controlling microstructural factors to achieve the required tensile properties of the dual-phase steels. The ANN model is expected to be useful in understanding the complex relationship between alloying elements, microstructural factors, and tensile properties in dual-phase steels.

Keywords: artificial neural network (ANN), dual-phase steels, alloying element, microstructural factor, tensile properties

1. Introduction

Over the past few decades, weight reductions and high strength levels of vehicle body structures have been the subjects of much research in order to improve fuel efficiency and safety in the automobile and transportation industries [1-8]. These demands have led to the development of advanced high strength steels (AHSS) that provide a weight reduction of about 25% compared to other conventional steels. Dual-phase steels are one of the most widely used AHSS with the excellent combination of strength and formability. Unlike conventional low-carbon steels, the dual-phase steels show continuous yielding, low yield-to-tensile strength ratio, and high work-hardening rate because they have a unique microstructure consisting of hard martensite in soft ferrite matrix [9-16]. However, it is difficult to predict the tensile properties of dual-phase steels because the microstructure varies depending on alloying elements or process conditions.

On the other hand, artificial neural networks (ANN) have been applied to predict various natural and social phenomena because they have many advantages in solving the complexity between the dependent and independent parameters [17-23]. The ANN techniques with these advantages have been increasingly used in materials science to design alloys and to predict mechanical properties. Recently, Reddy et al. [24] proposed an ANN model for predicting α and β phase volume fraction of

titanium alloys by controlling the chemical composition and heat-treatment process. Jung et al. [25] also investigated the effects of phase volume fraction on the tensile properties of high strength bainitic steels by using an ANN model. Although some researchers have applied the ANN model to predicting tensile properties, few ANN studies have considered both alloying elements and microstructural factors as input parameters to predict tensile properties.

In the present study, we developed an ANN model to predict the tensile properties of dual-phase steels by simultaneously considering alloying elements and microstructural factors as input parameters. Based on the developed ANN model, 3D contour maps and an average index of the relative importance were calculated to estimate the effects of the input parameters quantitatively on the yield strength, tensile strength, and yield-to-tensile ratio.

2. Artificial neural network modeling

For ANN and multiple linear regression modeling, experimental data were sourced from the literature on dual-phase steels with equiaxed morphology [26-30]. From the datasets, alloying elements (C, Mn, Si) and microstructural factors (martensite volume fraction, ferrite grain size) comprised input parameters, while tensile properties such as yield strength, tensile strength,

[1] SEOUL NATIONAL UNIVERSITY OF SCIENCE AND TECHNOLOGY, DEPARTMENT OF MATERIALS SCIENCE AND ENGINEERING, SEOUL, 01811, REPUBLIC OF KOREA

* Corresponding author: bhwang@seoultech.ackr

and yield-to-tensile ratio were output parameters. The input and output parameters were normalized within the range of 0.1 to 0.9 for this ANN model, using the relationship as below [20,21]:

$$x_n = \frac{(x - x_{min})*0.8}{(x_{max} - x_{min})} + 0.1$$

where x_n is the normalized value of x; x_{max} and x_{min} are the maximum and minimum values of x, respectively, in all datasets. Once the best-trained network was found, all the transformed data were set back to their original values by the following equation [20,21]:

$$x = \frac{(x_n - 0.1)(x_{max} - x_{min})}{0.8} + x_{min}$$

In this study, the ANN model was established using a back-propagation algorithm, and the sigmoid function was used as an activation function. The ANN model consisted of five neurons in the input layer and three neurons in the output layer, as shown in Fig. 1. The ANN training model involved adjusting the weights associated with each connection between neurons until the calculated output for each input dataset was close to the corresponding experimental result. To determine the optimal architecture and ascertain the reliability of the ANN model, datasets were partitioned into training datasets and test datasets. The 67 available datasets were divided into 61 training datasets and 6 test datasets. The ranges of 67 input and output parameters are summarized in Table 1 [26-30].

The architecture of the ANN model included hidden layers and neurons, a momentum term, a learning rate, and the number of iterations. During the ANN training step, the optimum parameters for the network were determined based on the average training error in the output prediction (E_{tr}) of the trained data; this is expressed which was given as [22]

$$E_{tr}(y) = \frac{1}{N}\sum_{i=1}^{N}\left|(T_i(y) - O_i(y))\right|$$

where N is the number of datasets, T_i is the targeted output, and O_i is the calculated output. As a result of ANN training after fixing 70 neurons and three hidden layers with minimum mean error values, the momentum term, learning rate, and iterations were optimized to 0.4, 0.6, and 70000, respectively.

With the help of the developed model, we attempted to estimate the significance of each alloying element and microstructural factor on tensile properties using a method called the
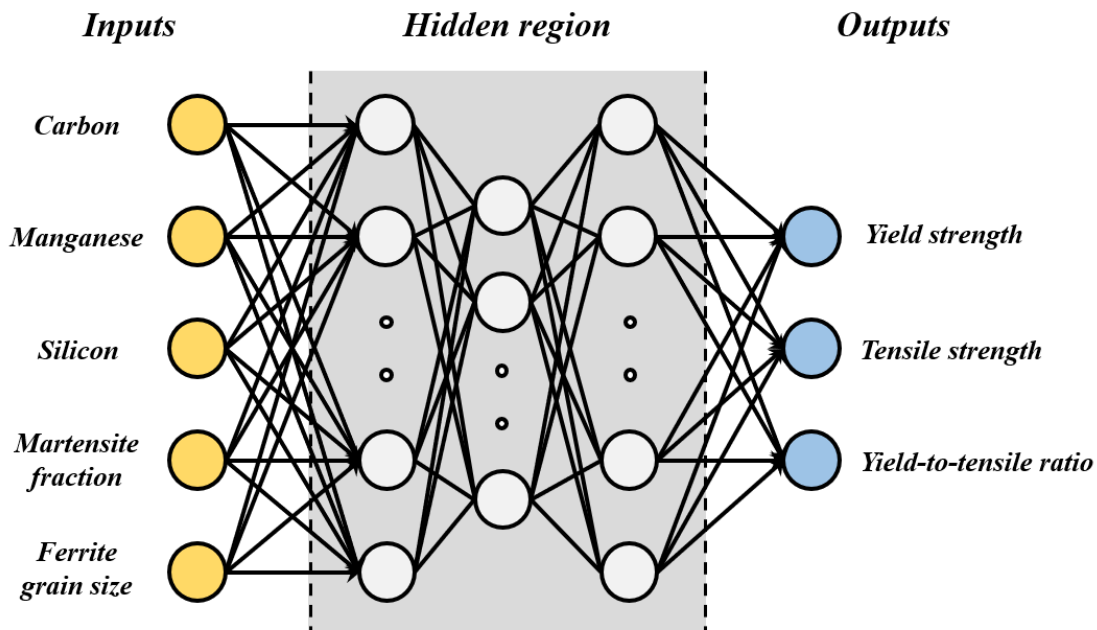

Fig. 1. Schematic model of the artificial neural network (ANN) architecture used to determine the tensile properties of dual-phase steels in this study

TABLE 1

The range of the input and output parameters for the ANN model [26-30]

	Parameter	Minimum	Maximum	Mean	Standard deviation
Input	C content (wt.%)	0.03	0.23	0.13	0.06
	Mn content (wt.%)	0.22	1.52	0.63	0.37
	Si content (wt.%)	0.01	0.45	0.12	0.12
	Martensite fraction (%)	2.60	95.00	32.03	18.56
	Ferrite grain size (μm)	2.25	91.00	21.92	19.02
Output	Yield strength (MPa)	172.40	755.70	401.48	121.18
	Tensile strength (MPa)	279.20	1089.70	729.61	230.83
	Yield-to-tensile ratio	0.39	0.88	0.57	0.13

index of relative importance (I_{RI}). The procedure to calculate the average index of the relative importance is given as follows.

(a) The % band of ith input parameter =
= $((X_1)\text{Maximum} - (X_1)\text{Minimum})/100$;

(b) The 6% band of each input parameter was considered i.e., +3% and −3%;

(c) As a result, input parameter X_1 has two row matrices $[+3\%X_1 + X_2 + X_3 + ... X_5]$ and $[-3\%X_1 + X_2 + X_3 + ... X_5]$

(d) When these two row matrices were passed through the ANN model, $(Y_1)_{+3\%X_1}$ and $(Y_1)_{-3\%X_1}$ were predicted.

(e) The difference, $\Delta(y_1) = (Y_1)_{+3\%X_1} - (Y_1)_{-3\%X_1}$ was calculated.

The index of relative importance (I_{RI}) of input parameter X_1 was calculated from the formula:

$$I_{RI} = \Delta(y_1)/((y_1)\text{Maximum} - (y_1)\text{Minimum})$$

3. Results and discussion

The performance of the ANN model was estimated by comparing the calculated values of the training data with the multiple linear regression results. As presented in Fig. 2(a-c), the tensile properties predicted by the ANN model had a high R^2 value of about 0.99 for the yield strength, tensile strength, and yield-to-tensile ratio. In contrast, the results predicted by the multiple linear regression model showed relatively low accuracy.

The ANN model was found to have a lower average percent error for all output parameters than the multiple linear regression model. Fig. 3 exhibits that the values predicted by the ANN model were more consistent with the experimental datasets than those predicted by the multiple linear regression model. It can be said that the developed ANN model predicts the yield strength, tensile strength, and yield-to-tensile ratio with remarkable accuracy.

On the other hand, the developed ANN model was applied to analyze the effect of multiple input parameters on yield strength, tensile strength, and yield-to-tensile ratio. From the analysis results of the developed ANN model, 3D contour maps were produced in Fig. 4. The martensite fraction and the ferrite grain size were set as parameters, and the Z-axis was also set as each tensile property (yield strength, tensile strength, and
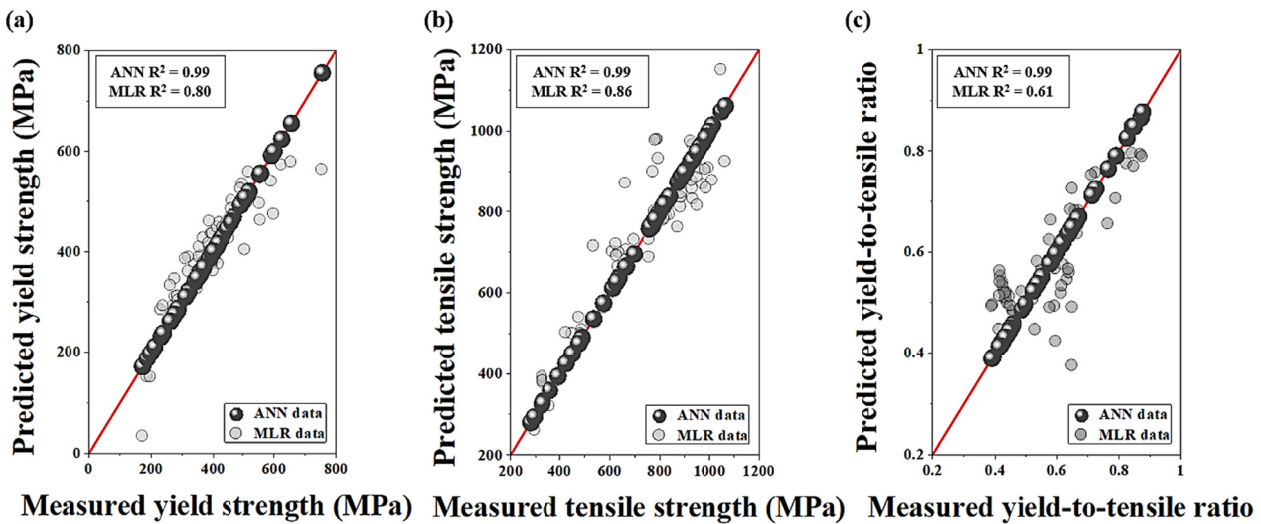

Fig. 2. Predictions of the artificial neural network (ANN) model and the multiple linear regression (MLR) model: (a) yield strength, (b) tensile strength, (c) and yield-to-tensile ratio
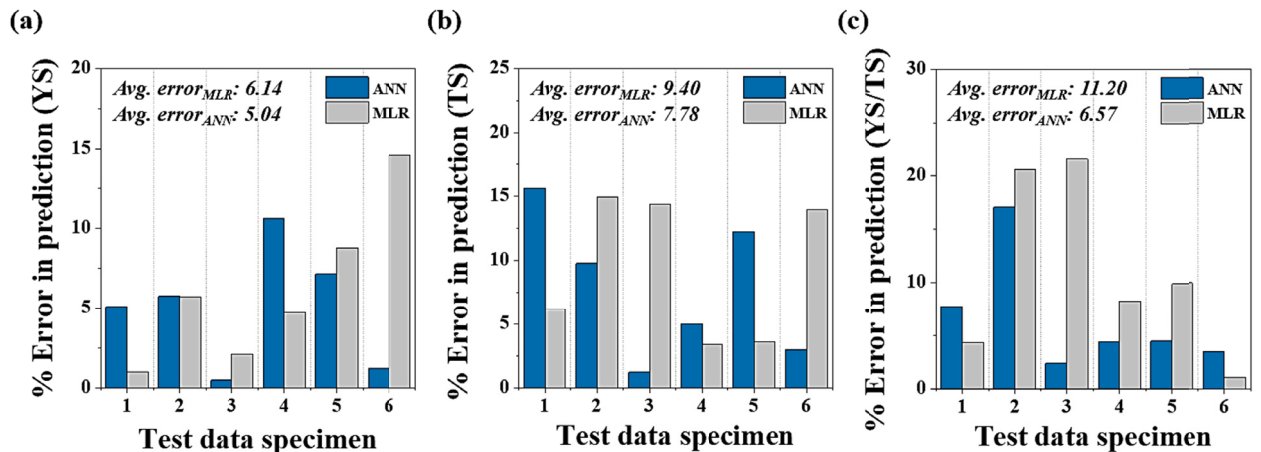

Fig. 3. Comparison of experimental and predicted tensile properties with the prediction error (%) for six test samples of dual-phase steel: (a) yield strength, (b) tensile strength, and (c) yield-to-tensile ratio
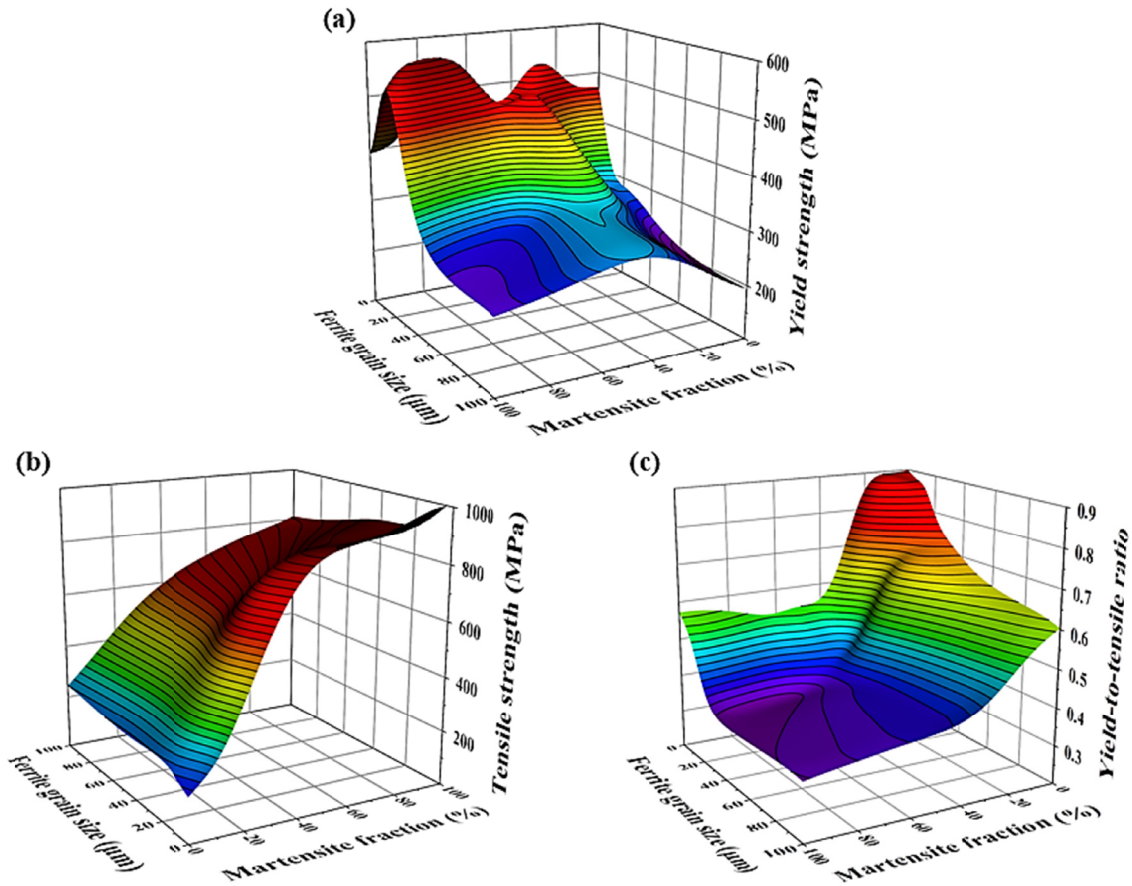
Fig. 4. 3D contour maps showing the combined effect of the martensite fraction and ferrite grain size on (a) yield strength, (b) tensile strength, and (c) yield-to-tensile ratio (dataset 36)

yield-to-tensile strength). The 3D contour maps demonstrated the influence of microstructural factors on the yield strength, tensile strength, and yield-to-tensile ratio in the dual-phase steel with a composition (C: 0.03, Mn: 0.02, Si: 0.01 wt.%). Fig. 4(a) shows variations in yield strength with different martensite fraction and ferrite grain size. The yield strength increased with a decrease in the ferrite grain size, and the martensite fraction had little effect on the yield strength. Unlike the yield strength, the tensile strength increased by the martensite fraction, and the ferrite grain

size showed an unclear tendency (Fig. 4(b)). Meanwhile, the yield-to-tensile ratio showed that the low yield-to-tensile ratio areas widen as the yield strength decreased, or tensile strength increased (Fig. 4(c)).

Fig. 5 exhibits the average index of the relative importance of the input parameters associated with the output parameters. The index was devised in the present study to compare the effects of the alloying elements and microstructural factors of input parameters quantitatively. For the average index of the relative
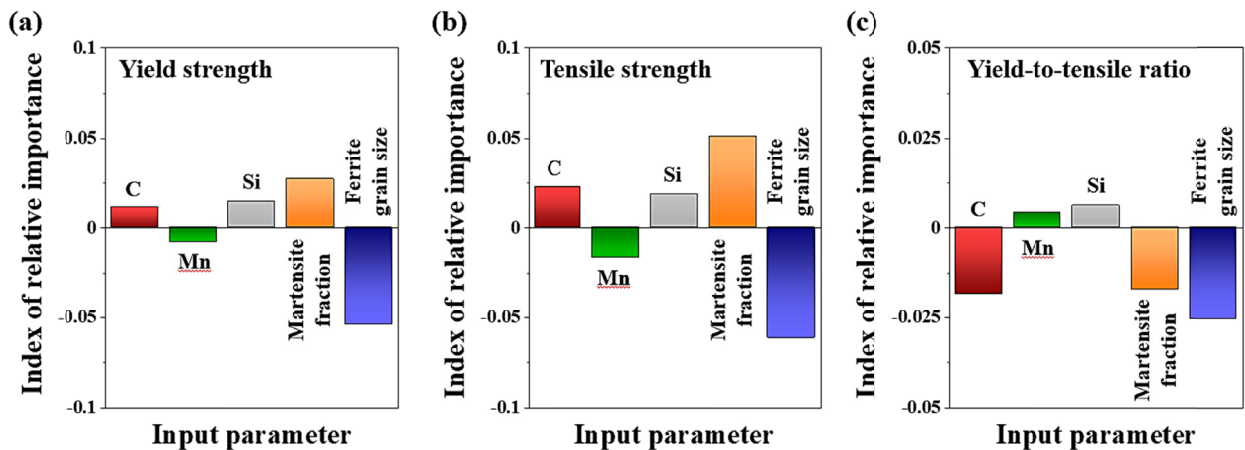

Fig. 5. The average index of the relative importance of the input parameters on the (a) yield strength, (b) tensile strength, and (c) yield-to-tensile ratio for all datasets

importance with reference to the yield and tensile strength (Fig. 5(a-b)), the martensite fraction had a positive influential factor, while the ferrite grain size had a negative influential factor. The other input parameters, i.e., the alloying elements, had insignificant influence. The yield-to-tensile ratio decreased at high tensile strength or low yield strength because it depends on both the martensite fraction and the ferrite grain size (Fig. 5(c)). From these results, it was found that microstructural factors had a greater impact on tensile properties than alloying elements.

4. Conclusions

1. The ANN model developed with consideration of both alloying elements and microstructural factors presented higher reliability than the multiple linear regression model for predicting the tensile properties of dual-phase steels.

2. The 3D contour maps and the average index of the relative importance calculated by the developed ANN model explained the complex effects of alloying elements and microstructural factors on the tensile properties of dual-phase steels.

3. The developed ANN model showed that martensite fractions and ferrite grain size had a greater impact on tensile properties than alloying elements, and thus it is important to control the microstructure when designing the desired tensile properties of dual-phase steels.

REFERENCES

[1] H.L. Kim, S.H. Bang, J.M. Choi, N.H. Tak, S.W. Lee, S.H. Park, Met. Mater. Int. **26**, 1757-1765 (2020).

[2] S.I. Lee, J. Lee, B. Hwang, Mater. Sci. Eng. **A 758**, 56-59 (2019).

[3] S.I. Lee, S.Y. Lee, J. Han, B. Hwang, Mater. Sci. Eng. **A 742**, 334-343 (2019).

[4] S.I. Lee, S.Y. Lee, S.G. Lee, H.G. Jung, B. Hwang, Met. Mater. Int. **24**, 1221-1231 (2018).

[5] S.Y. Lee, S.I. Lee, B. Hwang, Mater. Sci. Eng. **A 711**, 22-28 (2018).

[6] W. Bleck, S. Papaefthymiou, A. Frehn, Steel Res. Int. **75**, 704-710 (2004).

[7] M.J Jang, H. Kwak, Y.W Lee, Y.J. Jeong, J. Choi, Y.H. Jo, W.M. Choi, H.J. Sung, E.Y. Yoon, S. Praveen, S. Lee, B.J. Lee, M.I. Abd El Aal, H.S. Kim, Met. Mater. Int. **25**, 277-284 (2019).

[8] N. Saeidi, M. Jafari, J.G. Kim, F. Ashrafizadeh, H.S. Kim, Met. Mater. Int. **26**, 168-178 (2020).

[9] M. Soleimani, H. Mirzadeh, C. Dehghanian, Met. Mater. Int. **26**, 882-890 (2020).

[10] C.C. Tasan, M. Diehl, D. Yan, M. Bechtold, F. Roters, L. Schemmann, C. Zheng, N. Peranio, D. Ponge, M. Koyama, K. Tsuzaki, D. Raabe, Annual Rev. Mater. Res. **45**, 391-431 (2015).

[11] D. Das, P.P. Chattopadhyay, J. Mater. Sci. **44**, 2957-2965 (2009).

[12] D.K. Mondal, R.M. Dey, Mater. Sci. Eng. **A 149**, 173-181 (1992).

[13] M. Sarwar, R. Priestner, J. Mater. Sci. **31**, 2091-2095 (1996).

[14] B. Hwang, T. Cao, S.Y. Shin, S. Lee, S.J. Kim, Mater. Sci. Tech. **21**, 967-975 (2005).

[15] F. Najafkhani, H. Mirzadeh, M. Zamani, Met. Mater. Int. **25**, 1039-1046 (2019).

[16] J.I. Yoon, J. Jung, H.H. Lee, J.Y. Kim, H.S. Kim, Met. Mater. Int. **25**, 1161-1169 (2019).

[17] H. Duan, Y. Li, G. He, J. Zhang, Int. J. Mod. Phys. **B 23**, 1191-1196 (2009).

[18] S. Krajewski, J. Nowacki, Arch. Civ. Mech. Eng. **14**, 278-286 (2014).

[19] N.S. Reddy, C.H. Park, Y.H. Lee, C.S. Lee, Mater. Sci. Tech. **24**, 294-301 (2008).

[20] N.S. Reddy, Y.H. Lee, C.H. Park, C.S. Lee, Mater. Sci. Eng. **A 492**, 276-282 (2008).

[21] N.S. Reddy, B.B. Panigrahi, M.H. Choi, J.H. Kim, C.S. Lee, Comput. Mater. Sci. **107**, 175-183 (2015).

[22] N.S. Reddy, J. Krishnaiah, S.G. Hong, J.S. Lee, Mater. Sci. Eng. **A 508**, 93-105 (2009).

[23] T. Dutta, S. Dey, S. Datta, D. Das, Comput. Mater. Sci. **157**, 6-16 (2019).

[24] C. Lin, P.L. Nrayana, N.S. Reddy, S.W. Choi, J.T. Yeom, J.K Hong, C.H. Park, J. Mater. Sci. Tech. **35**, 907-916 (2019).

[25] I.D. Jung, D.S. Shin, D. Kim, J. Lee, M.S. Lee, H.J. Son, N.S. Reddy, M. Kim, S.K. Moon, K.T. Kim, J. Yu, S. Kim, S.J. Park, H. Sung, Materialia **11**, 100699 (2020).

[26] H.S. Lim, J.Y. Kim, B. Hwang, J. Korean. Soc. Heat Treat. **30**, 106-112 (2017).

[27] S. Sodjit, V. Uthaisangsuk, Mater. Des. **41**, 370-379 (2012).

[28] Z. Jiang, Z. Guan, J. Lian, Mater. Sci. Eng. **A 190**, 55-64 (1995).

[29] P. Chang, A.G. Preban, Acta Metall. **33**, 897-903 (1985).

[30] N.D. Beynon, S. Oliver, T.B. Jones, G. Fourlaris, Mater. Sci. Tech, **21**, 771-778 (2005).